Affinity Labeling of *Escherichia coli* Phenylalanyl-tRNA Synthetase at the Binding Site for $tRNA^{Phe}$ †

Codjo Hountondji, Jean-Marie Schmitter, Christian Beauvallet, and Sylvain Blanquet*
Laboratoire de Biochimie, Ecole Polytechnique, 91128 Palaiseau Cédex, France
Received November 3, 1986; Revised Manuscript Received March 5, 1987

ABSTRACT: Periodate-oxidized $tRNA^{Phe}$ ($tRNA_{ox}^{Phe}$) behaves as a specific affinity label of tetrameric *Escherichia coli* phenylalanyl-tRNA synthetase (PheRS). Reaction of the $\alpha_2\beta_2$ enzyme with $tRNA_{ox}^{Phe}$ results in the loss of $tRNA^{Phe}$ aminoacylation activity with covalent attachment of 2 mol of tRNA dialdehyde/mol of enzyme, in agreement with the stoichiometry of tRNA binding. Sodium dodecyl sulfate–polyacrylamide gel electrophoresis analysis of the PheRS–[^{14}C]$tRNA_{ox}^{Phe}$ covalent complex indicates that the large (α, M_r 87K) subunit of the enzyme interacts with the 3′-adenosine of $tRNA_{ox}^{Phe}$. The [^{14}C]tRNA-labeled chymotryptic peptides of PheRS were purified by both gel filtration and reverse-phase high-performance liquid chromatography. The radioactivity was almost equally distributed among three peptides: Met-Lys[Ado]-Phe, Ala-Asp-Lys[Ado]-Leu, and Lys-Ile-Lys[Ado]-Ala. These sequences correspond to residues 1–3, 59–62, and 104–107, respectively, in the N-terminal region of the 795 amino acid sequence of the α subunit. It is noticeable that the labeled peptide Ala-Asp-Lys-Leu is adjacent to residues 63–66 (Arg-Val-Thr-Lys). The latter sequence was just predicted to resemble the proposed consensus tRNA CCA binding region Lys-Met-Ser-Lys-Ser, as deduced from previous affinity labeling studies on *E. coli* methionyl- and tyrosyl-tRNA synthetases [Hountondji, C., Dessen, P., & Blanquet, S. (1986) *Biochimie 68*, 1071–1078].

Periodate-treated tRNA has recently emerged as a powerful affinity labeling reagent of aminoacyl-tRNA synthetases (Fayat et al., 1979; Hountondji et al., 1979, 1985, 1986a). The periodate treatment specifically oxidizes the 2′,3′-*cis*-diol function of the 3′-terminal ribose of tRNA. Inactivation and labeling of an aminoacyl-tRNA synthetase by oxidized tRNA ($tRNA_{ox}$) proceeds through the formation of a reversible Schiff base between the 2′,3′-aldehyde groups of $tRNA_{ox}$ and the ϵ-amino group of lysine residues inside the CCA binding site of tRNA on the enzyme. The equilibrium for Schiff base formation can be continuously and specifically displaced by reduction with sodium cyanoborohydride (Hountondji et al., 1979).

The use of oxidized tRNA to probe the active site of aminoacyl-tRNA synthetases is designated by the fact that positively charged side chains of the enzyme molecules, such as lysine residues, are expected to participate to the enzyme active center (Fayat et al., 1978) and/or to establish ionic bonds with phosphate groups of the polyanionic tRNA molecule, especially at its single-stranded 3′-acceptor end.

We have recently identified the peptides of *Escherichia coli* methionyl- and tyrosyl-tRNA synthetases labeled with their cognate oxidized tRNAs (Hountondji et al., 1985, 1986a). Comparison of these peptides to the known primary structures of several other aminoacyl-tRNA synthetases has indicated a sequence similarity among this family of enzymes, with a putative consensus sequence KMSKS (Hountondji et al., 1986b).

We now describe the specific labeling of the *E. coli* phenylalanyl-tRNA synthetase by periodate-treated $tRNA^{Phe}$. This enzyme comprises two different subunits arranged in the $\alpha_2\beta_2$ configuration (α, M_r 87 000, and β, M_r 37 000) (Fayat et al., 1974, 1983; Mechulam et al., 1985). Both types of subunit are required for the $tRNA^{Phe}$ aminoacylation and the phenylalanine-dependent ATP–PP_i exchange activities, since none of the isolated subunits shows significant catalytic activity (Ducruix et al., 1983).

Affinity labeling of phenylalanyl-tRNA synthetase demonstrates that the large (α, M_r 87K) subunit of the enzyme is responsible for the binding of the acceptor-end of $tRNA^{Phe}$, in agreement with recent studies by Khodyreva et al. (1985) on the active site distribution within the *E. coli* phenylalanyl-tRNA synthetase subunits. It is noteworthy that identification of the labeled peptides of the synthetase enables us to bring some support to the validity of the above putative consensus sequence.

Materials and Methods

Materials

Homogeneous phenylalanyl-tRNA synthetase was purified from *E. coli* strain EM 20031 carrying the F32 episome (Fayat et al., 1974) or from the overproducing strain IBPC 1671 carrying plasmid DNA pB1 (Ducruix et al., 1983). Its molecular ratio and optical extinction coefficient at 280 nm were taken equal to 248K and 0.80 $cm^2 \cdot mg^{-1}$, respectively (Fayat et al., 1974, 1983; Mechulam et al., 1985). Isolated α (M_r 87 000) and β (M_r 37 000) subunits of PheRS[1] were prepared as in Ducruix et al. (1983). Their specific optical coefficients at 280 nm, as calculated from their amino acid compositions (Fayat et al., 1983; Mechulam et al., 1985), were 0.7 and 0.5 unit/mg of α and β subunits, respectively. For this calculation, molar extinction coefficients of 1380 and 5550 $M^{-1} \cdot cm^{-1}$ were used for tyrosine and tryptophan, respectively (Beaven &

† This work was supported by the Centre National de la Recherche Scientifique (UA 240).
* Correspondence should be addressed to this author.

[1] Abbreviations: Lys[Ado], N^{ϵ}-adenosyllysine; SDS–PAGE, sodium dodecyl sulfate–polyacrylamide gel electrophoresis; RPLC, reverse-phase high-performance liquid chromatography; PP_i, inorganic pyrophosphate; RNase A, ribonuclease A. Aminoacyl-tRNA synthetases are abbreviated as a three-letter code of their specific amino acid followed by RS; the one- and three-letter amino acid codes are those suggested by IUPAB–IUB Commission on Biochemical Nomenclature.

0006-2960/87/0426-5433$01.50/0

Holliday, 1952). Unfractionated tRNA was obtained from the pilot facilities of the Institut de Chimie des Substances Naturelles du CNRS (Gif-sur-Yvette, France). Phenylalanyl-specific tRNA (1.1 nmol of phenylalanine acceptance/A_{260} unit of tRNA) was from Boehringer (Mannheim). $tRNA_m^{Met}$ was purified from *E. coli* K12 strain EM 20031 carrying the F32 episome, by the procedure of Seno et al. (1968). $tRNA^{Leu}$ was from Subriden RNA (Washington, DC). $tRNA_f^{Met}$, $tRNA^{Tyr}$, and $tRNA^{Glu}$ were from Boehringer (Mannheim). tRNA concentration was calculated according to its specific absorption coefficient at 260 nm (Guéron & Leroy, 1978). [^{14}C]ATP (450 Ci/mol) was from the Commissariat à l'Energie Atomique (Saclay, France). Ribonuclease A, α-chymotrypsin, and phenylmethanesulfonyl fluoride were from Sigma.

Methods

Inactivation of Phenylalanyl-tRNA Synthetase. Phenylalanyl-tRNA synthetase (1 μM) was incubated at 37 °C with 5 μM $tRNA_{ox}^{Phe}$ [prepared as in Fayat et al. (1979)] in a reaction mixture containing 20 mM imidazole hydrochloride buffer (pH 8), 24% glycerol, 10 mM $MgCl_2$, and 2 mM sodium cyanoborohydride. At various times, 10-μL aliquots of the reaction mixture were diluted in imidazole hydrochloride buffer (pH 7.6) containing 10 mM 2-mercaptoethanol and 200 μg/mL bovine serum albumin and assayed for the phenylalanine-dependent isotopic ATP–PP_i exchange and $tRNA^{Phe}$ aminoacylation activities (Lawrence et al., 1973; Blanquet et al., 1974).

Stoichiometry of Labeling. [^{14}C]$tRNA^{Phe}$ (specific radioactivity 7000 counts·min^{-1}·nmol^{-1}) was obtained by enzymatic labeling at its 3′-end with [^{14}C]ATP, in the presence of tRNA nucleotidyltransferase as previously described (Fayat et al., 1979; Hountondji et al., 1985). The enzyme (4 μM) was incubated in the presence of 12 μM [^{14}C]$tRNA_{ox}^{Phe}$ in the same conditions as above. At various times, portions of the reaction mixture were withdrawn and assayed for enzymatic activity. In parallel, aliquots were submitted to ribonuclease A digestion (10 μg/mL) for 2 min. Incorporation within the enzyme of the ^{14}C radioactivity was followed by precipitation with 5% trichloroacetic acid (Fayat et al., 1979). Following ribonuclease treatment, only the [^{14}C]adenosine cross-linked to PheRS was trichloroacetic acid insoluble, as verified by control experiments with intact [^{14}C]$tRNA^{Phe}$ in the absence or presence of PheRS.

Polyacrylamide Gel Electrophoresis. Proteins were denaturated in 2% sodium dodecyl sulfate, 2.5 M urea, 10% 2-mercaptoethanol, and 10% glycerol (3 min at 90 °C) and analyzed on a 12.5% polyacrylamide gel in tris(hydroxymethyl)aminomethane–glycine buffer (pH 8.5) containing 0.1% sodium dodecyl sulfate (Laemmli, 1970) at 100 V for 1.5 h and then 300 V for 4 h. Staining was with Coomassie Brilliant Blue R-250 in methanol/acetic acid/water (50/10/40 v/v/v). After the gel was destained in the latter solvent, it was swelled in methanol/acetic acid/water (10/10/80 v/v/v) and then equilibrated with a 5% sodium salicylate solution, dried, and autoradiographed by using an X-ray film (Kodak Eastman) for 24 h.

Preparation and Purification of ^{14}C-Labeled Chymotryptic Peptides of Phenylalanyl-tRNA Synthetase. Phenylalanyl-tRNA synthetase (35 mg) at a concentration of 3.2 mg/mL (13 μM) was incubated at 37 °C with 26 μM [^{14}C]$tRNA_{ox}^{Phe}$ in the same buffer conditions as above. The [^{14}C]adenosine incorporation into the enzyme was followed by submitting aliquots to ribonuclease digestion and trichloroacetic acid precipitation. At time 200 min, when 1.35 mol of ^{14}C was incorporated per mole of enzyme, the reaction was quenched by the addition of 25 mM $NaBH_4$ and the reaction mixture was dialyzed overnight against 4 L of 0.1 M NH_4HCO_3 (pH 8.2). The dialysate was incubated with chymotrypsin (40 μg/mg of PheRS) in the same buffer for 4 h at 37 °C. Proteolysis was stopped by the addition of phenylmethanesulfonyl fluoride at a final concentration of 0.5 mM, and the solution was freeze-dried.

Purification of the Labeled Peptides. Peptide purification from the PheRS–[^{14}C]$tRNA^{Phe}$ covalent complex was performed by a two-step chromatography on Sephadex G-50 as described in Hountondji et al. (1985, 1986a). The chymotryptic digest of the complex was loaded onto a first column of Sephadex G-50 in order to separate the tRNA-labeled peptides from the bulk of smaller unlabeled ones. The radioactive fractions from this step were pooled and treated with ribonuclease A prior to a second chromatography on Sephadex G-50. The latter purification step separated the [^{14}C]-adenosine-labeled peptides from the large unlabeled ones. Peptides containing the [^{14}C]label were finally purified in two steps by reverse-phase high-performance liquid chromatography (RPLC) on a Merck Superspher RP18 column (250 × 4 mm, 4-μm particles, 100-Å pore size) in a gradient elution mode. The first step removed most of the optical density, along with 8% of the applied radioactivity, close to the void volume of the RPLC column. The majority of the labeled material (77% of the applied radioactivity) was recovered with a steep gradient profile, pooled, and rechromatographed. The second RPLC step separated labeled peptides in a 2-h gradient run (Figure 7). Solvent A was 1 mM ammonium formate (pH 4.4), and solvent B was 20% A in methanol (Reinbolt et al., 1983). Detection was by dual-wavelength absorbance monitoring at 220 and 260 nm and by liquid scintillation counting of aliquots.

Sequence Analysis. Automated Edman degradation was carried out on a gas-phase sequencer (Applied Biosystems Model 470A). Samples were applied in 30-μL aliquots to glass fiber filters that had been previously treated with 3 mg of Polybrene and submitted to three precycles. Phenylthiohydantoin-amino acids (PTHs) were identified by RPLC online with the sequencer (unpublished results) by means of an isocratic system previously described by Lottspeich (1985). The column was a Merck Superspher RP8 (250 × 4 mm, 4-μm particles, 60-Å pore size). At each cycle, an amount of 40% of the formed PTH was analyzed by RPLC, the remaining part being counted for ^{14}C radioactivity.

RESULTS

Inactivation and Labeling with $tRNA_{ox}^{Phe}$. As shown in Figure 1, the $tRNA^{Phe}$ aminoacylation activity of phenylalanyl-tRNA synthetase (1 μM) markedly decreases upon incubation with oxidized $tRNA^{Phe}$ (5 μM), while the isotopic [^{32}P]PP_i–ATP exchange activity remains constant. The kinetics of inactivation fit a single-exponential curve with a rate constant of inactivation of 0.018 min^{-1} and a residual activity of 12 ± 3% (Figure 1). Oxidized bulk *E. coli* tRNA at a concentration of 250 μM, containing 2% of $tRNA^{Phe}$, also inactivates 1 μM of the enzyme with a rate constant identical with that observed with pure $tRNA_{ox}^{Phe}$ (Figure 1). This suggests that only the phenylalanine-specific component of the total tRNA specifically reacts with phenylalanyl-tRNA synthetase. Also, oxidized pure *E. coli* $tRNA^{Leu}$, $tRNA^{Glu}$, $tRNA^{Tyr}$, $tRNA_f^{Met}$, and $tRNA_m^{Met}$ (10 μM) were shown to not affect the activity of PheRS (1.4 μM).

Protection with $tRNA^{Phe}$. Intact $tRNA^{Phe}$ (16 μM) protects the enzyme (0.5 μM) against the inactivation by $tRNA_{ox}^{Phe}$ (5

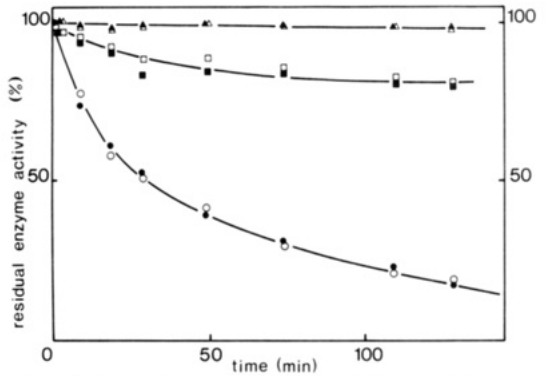

FIGURE 1: Kinetics of inactivation of phenylalanyl-tRNA synthetase by $tRNA_{ox}^{Phe}$. Experiments were performed as under Methods. The enzyme (1 μM) was incubated in the presence of 5 μM $tRNA_{ox}^{Phe}$ (●, ■) or 250 μM bulk $tRNA_{ox}$ (○, □). Residual tRNA aminoacylation (●, ○) and isotopic [^{32}P]PP_i–ATP exchange (■, □) activities are plotted vs. the time of incubation. Control experiments were performed without $tRNA_{ox}$ (▲) or with intact $tRNA^{Phe}$ (5 μM) instead of the dialdehyde (△).

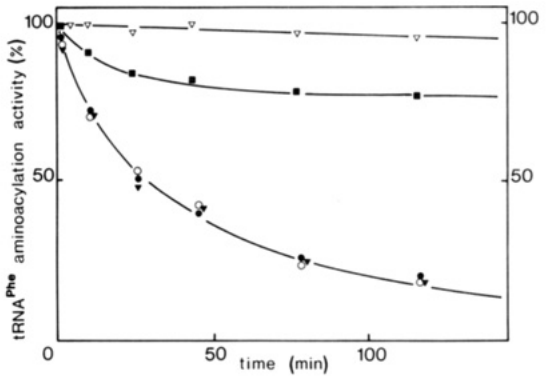

FIGURE 2: Effect of intact $tRNA^{Phe}$ and isolated α and β subunits of phenylalanyl-tRNA synthetase on inactivation of the enzyme by $tRNA_{ox}^{Phe}$. The enzyme (0.5 μM) was incubated with $tRNA_{ox}^{Phe}$ (5μM) in the presence (■) or absence (▼) of 16 μM intact $tRNA^{Phe}$ or in the presence of 0.7, 3.5, or 10 μM pure α subunit (●) or 1.7, 3.5, or 17 μM β subunit (○). A control experiment without $tRNA_{ox}$ (▽) is also shown.

μM) (Figure 2). In contrast, when added in the incubation mixture, neither the large (α, 10 μM) nor the small (β, 17 μM) isolated subunit of PheRS is able to afford protection (Figure 2). It can be therefore concluded that they do not compete with the native $\alpha_2\beta_2$ structure (0.5 μM) for $tRNA_{ox}^{Phe}$ fixation (5 μM).

Stoichiometry of Labeling. One mole of $\alpha_2\beta_2$ phenylalanyl-tRNA synthetase is fully inactivated by the incorporation of 1.90 ± 0.05 mol of [^{14}C]$tRNA_{ox}^{Phe}$ (Figure 3). This result is in satisfying agreement with the 1:2 enzyme:tRNA stoichiometry determined by solution light scattering (Holler et al., 1981) and small-angle neutron scattering (Dessen et al., 1983). Finally, the ^{14}C-labeled subunits of PheRS were identified by SDS–PAGE analysis (Figure 4). The enzyme was allowed to covalently bind to [^{14}C]$tRNA_{ox}^{Phe}$, and then, the PheRS–[^{14}C]$tRNA^{Phe}$ covalent complex was treated with ribonuclease A prior to polyacrylamide gel electrophoresis. It turns out that only the large subunit (α, M_r 87K) has reacted with the 3′-adenosine dialdehyde derivative of $tRNA^{Phe}$.

Peptide Purification. The enzyme (140 nmol) inactivated by [^{14}C]$tRNA_{ox}^{Phe}$ was reduced with sodium borohydride and digested with chymotrypsin. In order to counterselect the tRNA-labeled chymotryptic peptides from the unlabeled ones, the digest was fractionated by size exclusion chromatography (two consecutive separations on Sephadex G-50), as previously described (Hountondji et al., 1985, 1986a).

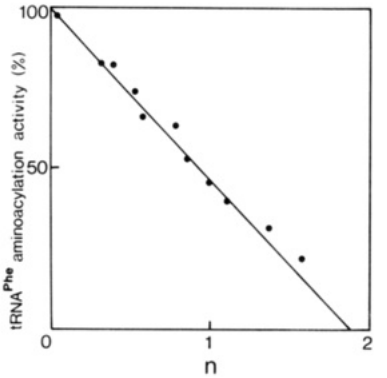

FIGURE 3: Stoichiometry of labeling of phenylalanyl-tRNA synthetase by [^{14}C]$tRNA_{ox}^{Phe}$. The enzyme (4 μM) was incubated with 12 μM [^{14}C]$tRNA_{ox}^{Phe}$ as under Methods. Incorporation into the enzyme of the 3′-[^{14}C]adenosine from [^{14}C]$tRNA_{ox}^{Phe}$ was followed by trichloroacetic acid precipitation after ribonuclease A digestion of aliquots of the incubation mixture. The number of [^{14}C]$tRNA_{ox}^{Phe}$ molecules (n) incorporated per mole of PheRS is represented as a function of the residual tRNA aminoacylation activity (%). A control experiment with intact [^{14}C]$tRNA^{Phe}$ showed no incorporation of radioactivity.

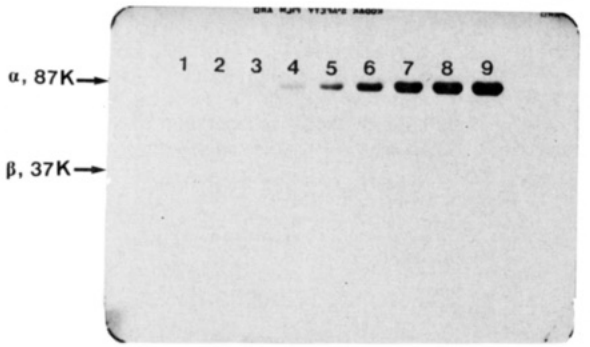

FIGURE 4: Identification by SDS–PAGE analysis of the subunit of phenylalanyl-tRNA synthetase involved in the covalent fixation of [^{14}C]$tRNA_{ox}^{Phe}$. Portions of the incubation mixture containing 4 μM PheRS and 12 μM [^{14}C]$tRNA_{ox}^{Phe}$ were withdrawn at various times of the kinetics of inactivation. After reduction with 25 mM $NaBH_4$, the portions were treated with ribonuclease A (100 μg/mL), denaturated with sodium dodecyl sulfate, and applied to a 12.5% polyacrylamide gel as described under Methods. The [^{14}C]adenosine-labeled protein was revealed by autoradiography. Lane 1, enzyme alone; lanes 2, 3, 4, 5, 6, 7, 8, and 9, portions incubated 0.5, 10, 20, 30, 45, 80, 115, and 200 min, respectively, in the prescence of [^{14}C]$tRNA_{ox}^{Phe}$. The arrows indicate the positions of the α (M_r 87K) and β (M_r 37K) subunits of PheRS, as revealed by the Coomassie Brilliant Blue staining of the same gel.

[^{14}C]tRNA-labeled peptides eluted as a single peak from the first G-50 column (Figure 5). After treatment with ribonuclease A, they were loaded on a second Sephadex G-50 column (Figure 6). Radioactivity representing [^{14}C]-adenosine-labeled peptides was recovered, and the corresponding material was then separated by two successive RPLC steps (cf. Methods). The chromatogram obtained with the second RP18 chromatography is shown in Figure 7; the overall yield of this chromatographic step was 85%, as estimated by radioactivity counting. A total of 78.4% of the recovered radioactivity was found in peaks I–X (Table I) which were submitted to N-terminal microsequencing; the remaining part (21.6%) was distributed on minor peaks that were not in sufficient amount for sequencing. ^{14}C-Labeled peptides were peaks I–III. Peaks I and III were pooled and directly sequenced, while peak II was rechromatographed on the RPLC column prior to sequencing.

As shown on the profile in Figure 7, peaks V and VII–X were clearly associated with radioactivity although they did not contain any significant amount of peptidic material. The

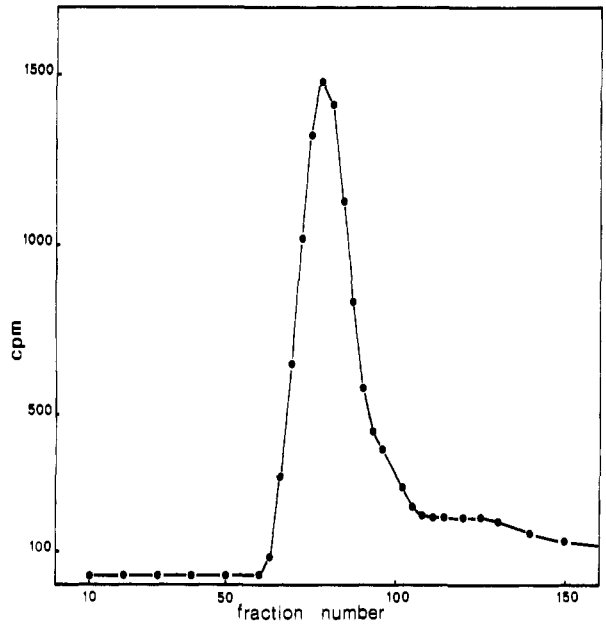

FIGURE 5: Gel filtration of the chymotryptic digest of the PheRS-[^{14}C]tRNA$_{ox}^{Phe}$ complex (8×10^5 cpm) on a column of Sephadex G-50 superfine (80×1.2 cm) in 0.1 M ammonium acetate (pH 8.2). The flow rate was 9 mL/h, and fractions of 0.45 mL were collected. A 20-μL aliquot from each fraction was counted for ^{14}C radioactivity. Fractions 63–105 were pooled and lyophilized.

Table I: Distribution of Radioactivity in the RPLC Separation of [^{14}C]tRNA-Labeled PheRS Chymotryptic Digest[a]

	radioactivity			radioactivity	
peak no.	cpm	%	peak no.	cpm	%
I	7000	14	VII	2600	5.2
II	5000	10	VIII	4200	8.4
III	6000	12	IX	2600	5.2
IV	1400	2.8	X	3400	6.8
V	3400	6.8	others (combined)	10800	21.6
VI	3600	7.2			

[a] For each radioactive peak (I–X) along the gradient profile of Figure 7, the corresponding 1-mL fraction was taken and counted for ^{14}C. Corresponding cpm values are given. The percentage is the ratio of the cpm in each peak to the total radioactivity eluted from the RPLC column (50 000 cpm).

radioactivity under peaks IV and VI, if any, could be overestimated by that of peaks I and II, respectively. If one supposes that the RNase action was total prior to the RPLC analysis, these peaks should originate from the part of the RNase A digested tRNA$_{ox}^{Phe}$ (32%) that had not reacted with enzyme under the conditions of the labeling experiment for peptide determination (see Methods). To test this possibility, a sample of [^{14}C]adenosine$_{ox-red}$, the expected product of the [^{14}C]tRNA$_{ox-red}$ digestion by RNase A, was submitted to RPLC analysis. Two-thirds of the radioactivity applied was recovered between 50 and 120 min of the gradient, in the form of several peaks. The locations of the three major peaks coincided with those of the above peaks VI, VIII, and X, thus confirming, at least partly, the origin of these peaks. The appearance of several peaks upon RPLC of a supposedly homogeneous $NaBH_4$-reduced [^{14}C]adenosine$_{ox}$ sample is difficult to explain. The complexity of the hydration of the dialdehyde group in aqueous solution can be invoked (Lowe & Beechey, 1982). In addition, intramolecular reactions such as Schiff base formation with the 6-NH_2 function of adenine have to be envisaged. In this context, it is also possible that, in the experiment involving tRNA, the terminal oxidized adenosine had reacted with the 4-amino group of the penultimate cytidine residue, changing the product of the RNase

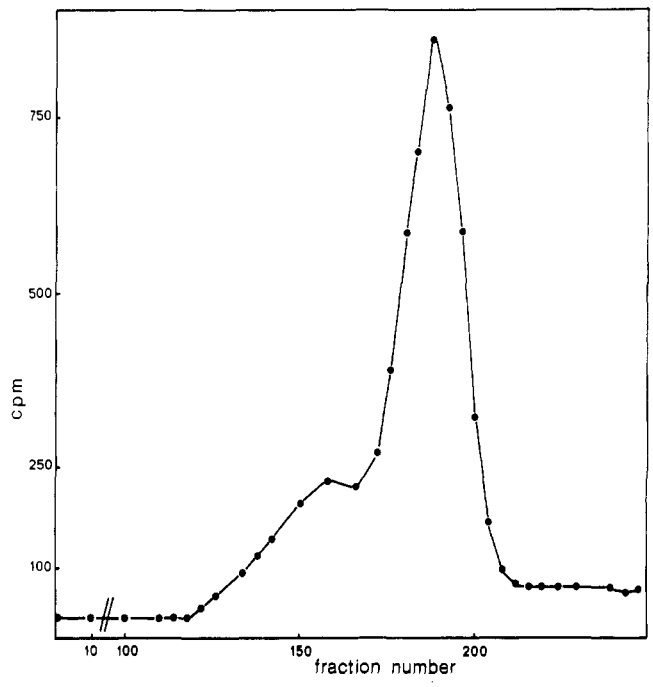

FIGURE 6: Chromatography on Sephadex G-50 superfine of the ribonuclease digest of the [^{14}C]tRNA^{Phe}-labeled peptides from Figure 5. The pooled radioactive material from Figure 5 was treated with ribonuclease A (160 μg/mL in 50 mM ammonium acetate, pH 8.2, 1 h, at 37 °C) and loaded onto a column of Sephadex G-50 superfine (55×1.2 cm) which was equilibrated and run with 50 mM ammonium acetate (pH 8.2). The flow rate was 3.6 mL/h, and fractions of 0.26 mL were collected. A 10-μL aliquot from each fraction was counted for ^{14}C radioactivity. Fractions 120–210 were pooled and lyophilized.

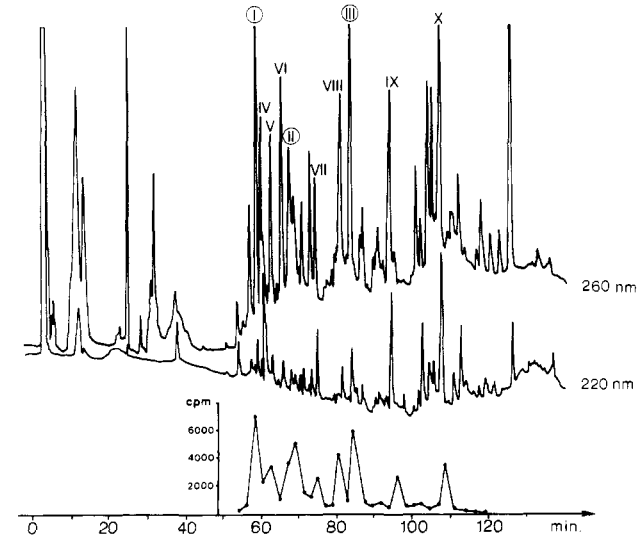

FIGURE 7: RPLC separation on a RP18 Superspher column of [^{14}C]adenosine-labeled peptides from Figure 6. Shown is the dual-wavelength detection at 260 [0.01 absorbance unit full scale (AUFS), upper trace] and 220 nm (0.05 AUFS), as well as the total ^{14}C radioactivity (cpm) within each collected fraction (1 mL). Solvent A was 1 mM ammonium formate (pH 4.4). Solvent B was 20% A in methanol. Flow rate was 0.5 mL/min with a multilinear gradient from 0% to 100% B in 120 min (cf. Methods). Radioactive peaks I–X were applied on the sequencer (cf. Table I). ^{14}C-Labeled peptides were peaks I–III (cf. Table II). Nonradioactive light-absorbing peaks (not numbered) were not sequenced.

A action into a dinucleoside instead of the expected 3′-adenosine, and thus accounting for additional peaks on the RPLC profile.

Peptide Sequence. The amino acid sequences of chymotryptic peptides I–III were compared to the primary structure of *E. coli* phenylalanyl-tRNA synthetase (Fayat et al., 1983;

Table II: N-Terminal Sequencing of the Radioactive Peptides[a]

cycle no.	residue no. in the sequence of PheRS	amino acid	radioactivity (cpm)	yield of PTH (pmol)
		Peptide I		
1	59	Ala	90	135
2	60	Asp	60	105
3	61	Lys[Ado]	610	75
4	62	Leu	210	50
		Peptide II		
1	104	Lys	95	115
2	105	Ile	80	105
3	106	Lys[Ado]	480	65
4	107	Ala	260	80
		Peptide III		
1	1	Met	80	110
2	2	Lys[Ado]	440	60
3	3	Phe	190	95

[a] About 200 pmol of each of peptides I, II, or III was sequenced. The cycles were counted for ^{14}C radioactivity and analyzed for phenylthiohydantoin-amino acids (PTH-amino acids), as described under Methods.

Mechulam et al., 1985). Peptides I, II, and III coincide with positions 59–62 (-Ala-Asp-Lys-Leu-), 104–107 (-Lys-Ile-Lys-Ala-), and 1–3 (Met-Lys-Phe-), respectively, from the amino terminus of the amino acid sequence of the large (α, M_r 87K) subunit of the enzyme (Table II) (Mechulam et al., 1985). In the automated Edman degradation (Table II), the radioactivity from the labeled peptides was recovered in a phenylthiohydantoin (PTH) that eluted from the RP8 column close to PTH-histidine. This was assumed to be the PTH derivative of [^{14}C]adenosyllysine. The retention time of PTH-Lys[Ado] with this chromatographic system was ascertained by the Edman degradation of a known [^{14}C]-adenosine-labeled peptide whose amino acid sequence was previously established by using a Beckman 890C liquid–phase sequencer (Hountondji et al., 1986a) (results not shown). Thus, the labeled lysine residues were Lys-61 (peptide I), Lys-106 (peptide II), and Lys-2 (peptide III). They account for 36% of the radioactivity eluted from the RPLC column.

Discussion

Affinity labeling of *E. coli* phenylalanyl-tRNA synthetase by $tRNA_{ox}^{Phe}$ yields a specific 1:2 covalent complex, in agreement with the known binding of 1 mol of PheRS ($\alpha_2\beta_2$) to 2 mol of intact $tRNA^{Phe}$ (Dessen et al., 1983). The $tRNA^{Phe}$ aminoacylation activity of the enzyme is destroyed by the labeling, while the phenylalanine-dependent isotopic [^{32}P]-PP_i–ATP exchange activity is not significantly changed. It is reminiscent of the case of PheRS from *Saccharomyces cerevisiae* where, similarly, only the tRNA aminoacylation activity was affected by the covalent attachment of $tRNA_{ox}$ to the enzyme (Baltzinger et al., 1979), but it contrasts with the loss of both enzymatic activities following covalent modification of homodimeric methionyl- and tyrosyl-tRNA synthetases by their specific $tRNA_{ox}$ (Fayat et al., 1979; Hountondji et al., 1985, 1986a). Such a discrepancy may reflect the different structural organizations of the binding sites for ATP, amino acid, and tRNA on synthetases having extremely different molecular weights and subunit compositions.

Under our experimental conditions, only the large (α) subunit of *E. coli* PheRS interacts with the 3′-acceptor end of $tRNA^{Phe}$, provided that this subunit is combined to the β subunit in the native structure of the enzyme. This result agrees well with previously reported affinity labeling studies that showed the covalent binding of *N*-(bromoacetyl)-phenylalanyl-$tRNA^{Phe}$ to the large subunit of PheRS (Bartmann et al., 1974; Khodyreva et al., 1985).

From the chymotryptic digest of the covalent PheRS–[^{14}C]$tRNA_{ox}^{Phe}$ complex, three peptides were isolated by means of RPLC. The corresponding [^{14}C]adenosine-labeled lysine residues are Lys-2, Lys-61, and Lys-106, located in the N-terminal part of the primary structure of the large (α) subunit of the enzyme (Mechulam et al., 1985). To our knowledge, this is the first evidence in favor of the participation of the N-terminal region of an aminoacyl-tRNA synthetase in the binding of the CCA arm of tRNA. It is even more striking that the N-terminal sequence (Met-Lys-Phe-) itself seems to be close to the 3′-end of enzyme-bound tRNA and may be involved in its recognition. Such features differ from the cases of alanyl- and tyrosyl-tRNA synthetases (homotetramer and dimer, respectively), whose N- and C-terminal parts would be responsible for the ATP–PP_i exchange and tRNA aminoacylation reactions, respectively (Jasin et al., 1983; Waye et al., 1983). Such a discrepancy might reflect the unusual $\alpha_2\beta_2$ structure of PheRS.

The labeling of PheRS has identified three distinct lysines in the vicinity of the binding site for the 3′-end of tRNA. However, these three lysine residues are rather close to each other in the primary structure and, supposedly, clustered within the enzyme's three-dimensional (3-D) structure. It should be recalled that the same figures were encountered in *E. coli* MetRS and TyrRS, although these synthetases were converted into their specific 1:1 covalent complexes with cognate oxidized tRNAs (Hountondji et al., 1985, 1986a). In the case of MetRS, two major tRNA-labeled lysine residues (lysines-335 and -61) and three minor ones (lysines-142, -147, and -149) were identified, while, in the case of TyrRS, lysines-229, -234, and -237 could be labeled with $tRNA_{ox}^{Tyr}$. The reaction of distinct lysines of MetRS and TyrRS, when the tRNA binds a unique site at the surface of these synthetases, could be explained by the clustering of these lysines in the primary structure or the 3-D structure (Hountondji et al., 1986a), as well as by the flexibility of the protein structures and the mobility of the CCA end of the bound tRNA molecules. Finally, the observation that all three lysines of PheRS are equally modified in a mutually exclusive fashion while the enzyme activity is almost completely destroyed favors the conclusion that the modification of any lysine impairs the tRNA aminoacylation reaction or, in other words, that any identified lysine may play an important role in the tRNA binding process.

According to Khodyreva et al. (1985), who studied the localization of the substrate-binding sites on the subunits of *E. coli* phenylalanyl-tRNA synthetase, the binding sites for $tRNA^{Phe}$ and phenylalanyl-$tRNA^{Phe}$ are located on the large subunits of the enzyme while those for phenylalanine are on the small subunits and those for ATP and the aminoacyl moiety of phenylalanyl-tRNA are localized near the contact region between the subunits. These findings led these authors to propose that the tRNA aminoacylation active center was formed by the contact region of subunits. Consequently, we propose that the N-terminal region of the large subunits that comprises the labeled lysines-2, -61, and -106 makes a contact with the small subunits of the enzyme in the tertiary structure. In support of this idea, residues 1–110 of the large subunit of the enzyme have a rather hydrophobic character indicative of a buried environment for the labeled lysines (Hountondji et al., 1986b). Furthermore, the presence of the small subunits would be necessary for the correct geometry of the tRNA binding site on the large subunits, in agreement with the fact

that both subunits are required for enzyme activity (Ducruix et al., 1983) and with the observation in this study that the isolated α or β subunits cannot bind tRNA.

Recently, the comparison of the *E. coli* methionyl- and tyrosyl-tRNA synthetase sequences around the $tRNA_{ox}$-labeled lysine residues has indicated a sequence similarity (Hountondji et al., 1985, 1986a). On the basis of this observation, similar amino acid sequences were searched for in all the known primary structures of aminoacyl-tRNA synthetases. Interestingly, the sequence KMSKS was observed in a large number, but not all, of the aminoacyl-tRNA synthetases, and it was suggested that this amino acid sequence might constitute part of the CCA binding region of tRNA (Hountondji et al., 1986b). Taking into account that lysine, methionine, and serine are chemically similar to arginine, valine, and threonine, respectively, it was predicted that the sequence RVTK (positions 63–66) in the α subunit of PheRS resembles the consensus sequence KMSKS. It is striking that, in this study, one labeled peptide accounting for a third of the incorporation of $tRNA_{ox}^{Phe}$ is just adjacent to the expected sequence RVTK of PheRS. Although the tRNA-labeled Lys-61 is not the predicted Lys-66 residue, both lysines belong to the 11 amino acid stretch of PheRS that we found poorly similar to the CCA binding Lys-335 region of MetRS (Hountondji et al., 1986b). The proximity of lysines-61 and -66 in the primary structure of PheRS may imply that they are near each other in the 3-D structure of the enzyme. In fact, a similar situation was encountered with *E. coli* tyrosyl-tRNA synthetase, where the most reactive lysine was Lys-234, different from, but very close to, Lys-229, designated by the sequence comparison and which we found only partially labeled (Hountondji et al., 1986a). Thus, the present result brings some credibility to the KMSKS sequence as a possible diagnostic tool for localizing the CCA binding region of tRNA in the primary structure of a bacterial aminoacyl-tRNA synthetase, even if this consensus sequence does not permit to safely predict the lysine hit by the flexible end of $tRNA_{ox}$.

Besides phenylalanyl-tRNA synthetase, only one *E. coli* aminoacyl-tRNA synthetase has the unusual $\alpha_2\beta_2$ quaternary structure. This is glycyl-tRNA synthetase, an enzyme of M_r 218 000 with M_r of the α and β subunits equal to 35 000 and 76 000, respectively (Ostrem & Berg, 1974; McDonald et al., 1980; Webster et al., 1983). *E. coli* phenylalanyl- and glycyl-tRNA synthetases have in common many features: (i) both enzymes bind two molecules of their cognate tRNA per molecule of the $\alpha_2\beta_2$ structure (Holler et al., 1981; Dessen et al., 1983; Nagel et al., 1984; this work); (ii) the larger subunits of both enzymes play a major role in tRNA recognition (Bartmann et al., 1974; Nagel et al., 1984; Khodyreva et al., 1985; this work); (iii) both enzymes reversibly dissociate into subunits in the presence of 0.5 M NaSCN (McDonald et al., 1980; Ducruix et al., 1983); (iv) isolated subunits from both enzymes are unable to catalyze the ATP–PP_i exchange and the tRNA aminoacylation reactions (Ostrem & Berg, 1974; McDonald et al., 1980; Ducruix et al., 1983). Thus, one might expect a common active site distribution for these two aminoacyl-tRNA synthetases and, possibly, sequence similarities in the functional regions of their polypeptide chains. Toth and Schimmel (1986) used oligonucleotide-directed mutagenesis to fuse the carboxyl terminus of the small polypeptide chain to the amino terminus of the large chain of GlyRS and observed that the fusion did not completely destroy the activity of the enzyme. This observation may indicate that, in the native $\alpha_2\beta_2$ structure of GlyRS, the N-terminal region of the large subunit already lies close to the C-terminal region of the small subunit. This idea is in agreement with our above discussion concerning a putative contact between the amino terminus of the large subunit with the small subunit surface of PheRS and argues for similar structural organization between the two $\alpha_2\beta_2$ synthetases. On the other hand, no marked similarity could be observed at the level of the amino acid sequences of the two aminoacyl-tRNA synthetases (Fayat et al., 1983; Mechulam et al., 1985; Webster et al., 1983). Nevertheless, we found a very limited sequence similarity in the Lys-106 region of PheRS whose Lys-Ile-Lys-Ala peptide (positions 104–107) (Mechulam et al., 1985) is also present in the primary structure of the large subunit of GlyRS (positions 225–228) (Webster et al., 1983). This short amino acid sequence is precisely one of those identified in this study as a tRNA-cross-linked peptide. It might therefore represent a part of the tRNA site of GlyRS as well. Further studies are needed to explore this possibility.

ACKNOWLEDGMENTS

We thank Drs. Y. Mechulam, P. Dessen, and A. Ducruix for fruitful discussions and the reviewer of our manuscript for helpful criticisms.

Registry No. PheRS, 9055-66-7.

REFERENCES

Baltzinger, M., Fasiolo, F., & Rémy, P. (1979) *Eur. J. Biochem. 97*, 481–494.

Bartmann, P., Hanke, T., Hammer-Raber, B., & Holler, E. (1974) *Biochem. Biophys. Res. Commun. 60*, 743–747.

Beaven, G. H., & Holliday, E. R. (1952) *Adv. Protein Chem. 7*, 319–386.

Blanquet, S., Fayat, G., & Waller, J. P. (1974) *Eur. J. Biochem. 44*, 343–351.

Dessen, P., Ducruix, A., Hountondji, C., May, R. P., & Blanquet, S. (1983) *Biochemistry 22*, 281–284.

Ducruix, A., Hounwanou, N., Reinbolt, J., Boulanger, Y., & Blanquet, S. (1983) *Biochim. Biophys. Acta 741*, 244–250.

Fayat, G., Blanquet, S., Dessen, P., Batelier, G., & Waller, J. P. (1974) *Biochimie 56*, 35–41.

Fayat, G., Fromant, M., & Blanquet, S. (1978) *Proc. Natl. Acad. Sci. U.S.A. 75*, 2088–2092.

Fayat, G., Hountondji, C., & Blanquet, S. (1979) *Eur. J. Biochem. 96*, 87–92.

Fayat, G., Mayaux, J. F., Sacerdot, C., Fromant, M., Springer, M., Grunberg-Manago, M., & Blanquet, S. (1983) *J. Mol. Biol. 171*, 239–261.

Guéron, M., & Leroy, J. L. (1978) *Anal. Biochem. 91*, 691–694.

Holler, E., Wang, C. C., & Ford, N. C., Jr. (1981) *Biochemistry 20*, 861–867.

Hountondji, C., Fayat, G., & Blanquet, S. (1979) *Eur. J. Biochem. 102*, 247–250.

Hountondji, C., Blanquet, S., & Lederer, F. (1985) *Biochemistry 24*, 1175–1180.

Hountondji, C., Lederer, F., Dessen, P., & Blanquet, S. (1986a) *Biochemistry 25*, 16–21.

Hountondji, C., Dessen, P., & Blanquet, S. (1986b) *Biochimie 68*, 1071–1078.

Jasin, M., Regan, L., & Schimmel, P. (1983) *Nature (London) 306*, 441–447.

Khodyreva, S. N., Moor, N. A., Ankilova, V. N., & Lavrik, O. I. (1985) *Biochim. Biophys. Acta 830*, 206–212.

Laemmli, U. K. (1970) *Nature (London) 227*, 680–685.

Lawrence, F., Blanquet, S., Poiret, M., Robert-Gero, M., & Waller, J. P. (1973) *Eur. J. Biochem. 36*, 234–243.

Lottspeich, F. (1985) *J. Chromatogr. 326*, 321–327.

Lowe, P. N., & Beechey, R. B. (1982) *Bioorg. Chem. 11*, 55–71.
McDonald, T., Breite, L., Pangburn, K. L. W., Hom, S., Manser, J., & Nagel, G. M. (1980) *Biochemistry 19*, 1402–1409.
Mechulam, Y., Fayat, G., & Blanquet, S. (1985) *J. Bacteriol. 163*, 787–791.
Nagel, G. M., Cumberledge, S., Johnson, M. S., Petrella, E., & Weber, B. H. (1984) *Nucleic Acids Res. 12*, 4377–4384.
Ostrem, D. L., & Berg, P. (1974) *Biochemistry 13*, 1338–1348.
Reinbolt, J., Hounwanou, N., Boulanger, Y., Wittmann-Liebold, B., & Bosserhoff, A. (1983) *J. Chromatogr. 259*, 121–130.
Seno, T., Kobayashi, M., & Nishimura, S. (1968) *Biochim. Biophys. Acta 169*, 80–94.
Toth, M. J., & Schimmel, P. (1986) *J. Biol. Chem. 261*, 6643–6646.
Waye, M. M. Y., Winter, G., Wilkinson, A. J., & Fersht, A. R. (1983) *EMBO J. 2*, 1827–1829.
Webster, T. A., Gibson, B. W., Keng, T., Biemann, K., & Schimmel, P. (1983) *J. Biol. Chem. 258*, 10637–10641.

The Elasticity of Uniform, Unilamellar Vesicles of Acidic Phospholipids during Osmotic Swelling Is Dominated by the Ionic Strength of the Media

Thomas H. Haines,* Wei Li, Michael Green, and Herman Z. Cummins
Departments of Chemistry and Physics, The City College of The City University of New York, New York, New York 10031
Received December 2, 1986; Revised Manuscript Received February 9, 1987

ABSTRACT: Uniform, unilamellar vesicles have been prepared by the pH-modification technique. The initial sizes of the vesicles were from 200 to 700 nm and were measured to within 1–3% by photo correlation spectroscopy. Vesicles were made of the dioleoyl esters of phosphatidic acid, phosphatidylcholine, phosphatidylglycerol, phosphatidylethanolamine, the diphytanyl ethers of phosphatidylglycerol, *Escherichia coli* lipids, and lac permease reconstituted into *E. coli* lipids. The vesicle suspensions were prepared and then diluted with electrolyte (KCl) and/or nonelectrolyte (sucrose, trehalose, pentaerythritol) impermeants. The amplitude of the swelling is linearly proportional to the osmotic pressure difference across the bilayer. We have determined the elastic modulus, the elastic limit (percent surface expansion at bursting), and the transbilayer pressure difference at bursting for each of these vesicles at constant osmolarity but at different ionic strengths. We find that the elastic properties of the bilayer vary by a factor of 10 in electrolyte media as compared to isosmolal nonelectrolyte media and that this variation appears to be related to both the charge density at the surface and the ionic strength of the media. Anionic lipid vesicles in 150 mM KCl have a significantly higher modulus (50×10^7 dyn/cm^2) and transbilayer pressure difference (40 mosM) at bursting with a small capacity to stretch (3–4% surface expansion) compared to the same vesicles suspended in nonelectrolyte impermeants. The latter vesicles undergo a significant surface expansion (8–10%), display a low modulus (3×10^7 dyn/cm^2), and burst at 3–4 mosM bilayer pressure difference. Vesicles suspended in media of constant osmolarity at various ionic strengths display properties with proportional values. Vesicles burst when diluted from 150 to 120 ± 5 mM KCl or from 250 to 215 ± 5 mM sucrose. This is a considerably narrower range of dilutions than has been examined by studies on the effects of osmotic stress on bilayers in the literature. A comparison of the mechanical properties of bilayers comprised of different lipid head groups shows that dioleoylphosphatidylethanolamine displays the properties of an acidic lipid with an unusually high modulus, low surface expansion, and high transbilayer pressure difference at bursting. This contrasts with dioleoylphosphatidylserine, which displays an unusually low modulus, moderate surface expansion, and a low transbilayer pressure difference at bursting. Vesicles of reconstituted *E. coli* lactose carrier into the cell's lipids display an even higher modulus than phosphatidylethanolamine, which dominates the bacterium's lipid composition.

Vesicles of pure phospholipids have been used as models for an understanding of the properties of biological membranes since the early experiments of A. D. Bangham and his coworkers, who showed that synthetic phospholipids could form spontaneous bilayers (Bangham et al., 1965; Bangham, 1968, 1972) with osmotic properties (Bangham et al., 1967). Most of this work has been conducted on multilayered liposomes, a complicated system for studying osmotic swelling as has recently been shown by comparing the osmotic properties of standard preparations of open-ended rolls to multilamellar closed concentric spheres made by a new preparation procedure (Gruner et al., 1986). Very recently, osmotic studies have been conducted on unilamellar vesicles including giant vesicles (10 μm) (Kwok & Evans, 1981) of DMPC, sonicated (SUV)[1]

* Address correspondence to this author at the Department of Chemistry.

[1] Abbreviations: BLM, bilayer lipid membrane; ΔP, transbilayer pressure difference at bursting; DMPC, 1,2-dimyristoyl-3-*sn*-glycerophosphocholine; DOPA, 1,2-dioleoyl-3-*sn*-phosphatidic acid; DOPC, 1,2-dioleoyl-3-*sn*-phosphatidylcholine; DOPE, 1,2-dioleoyl-3-*sn*-phosphatidylethanolamine; DOPG, *rac*-1,2-dioleoyl-3-*sn*-phosphatidylglycerol; DΦPC, diphytanoylphosphatidylcholine; DΦPG, diphytanylphosphatidylglycerol; EM, electron microscope; EPC, egg phosphatidylcholine; HDTA, hexadecyltrimethylammonium chloride; Hepes, *N*-(2-hydroxyethyl)piperazine-*N*′-2-ethanesulfonic acid; LUV, large unilamellar vesicles; MDO, membrane-derived oligosaccharides; PCS, photon correlation spectroscopy; SUV, sonicated (small) unilamellar vesicles; TLC, thin-layer chromatography; Tris-HCl, tris(hydroxymethyl)aminomethane hydrochloride.

0006-2960/87/0426-5439$01.50/0